Structural basis and specificity of human otubain 1 mediated deubiquitylation

[1,6]Mariola J. Edelmann, [1,6]Alexander Iphoefer, [3]Masato Akutsu, [1]Mikael Altun, [2]Katalin di Gleria, [1]Holger B. Kramer, [4]Edda Fiebiger, [3,5]Sirano Dhe-Paganon and [1,5]Benedikt M. Kessler

[1]Henry Wellcome Building for Molecular Physiology, Department of Clinical Medicine, Roosevelt Drive, [2]Weatherall Institute of Molecular Medicine, University of Oxford, OX3 7BN Oxford, UK
[3]Structural Genomics Consortium and the Department of Physiology, University of Toronto, Ontario, M5G 1L5, Canada
[4]Department of Gastroenterology/Nutrition, Children's Hospital, Boston MA 02115, USA

[5]Corresponding authors: Benedikt Kessler
University of Oxford
Phone: +44 1865 287 799
Fax: +44 1865 287 804
Email: bmk@ccmp.ox.ac.uk

Sirano Dhe-Paganon
SGC, University of Toronto
Phone: +1 416 946 3876
Email: sirano.dhepaganon@utoronto.ca

[6]These authors contributed equally to this work

Running Title: Structural insights into human otubain 1

Key words: Crystal structure; deubiquitylating enzyme; DUB, ISG15; NEDD8; otubain 1; OTUB1; SUMO; ubiquitin

Abbreviations: FUS/TLS: fusion involved in t(12:16) in malignant liposarcoma / translocation in liposarcoma; ; LC-MS/MS: liquid chromatography tandem mass spectrometry; OTUB1: otubain 1; OTUB2: otubain 2; Rack 1: receptor for activated kinase 1; Ub: ubiquitin

Word counts: Total: 8121; Abstract: 191

Abstract

Otubain 1 (OTUB1) is a human deubiquitylating enzyme implicated in mediating lymphocyte antigen responsiveness, but whose molecular function is generally not well defined. A structural analysis of OTUB1 shows differences in accessibility to the active site and in surface properties of the substrate binding regions when compared with its close homologue, otubain 2 (OTUB2), suggesting variations in regulatory mechanisms and substrate specificity. Biochemical analysis reveals that OTUB1 has a preference for cleaving lys^{48}- over lys^{63}-linked poly-ubiquitin chains, and it is capable of cleaving NEDD8, but not SUMO1/2/3 and ISG15 conjugates. A functional comparison of OTUB1 and OTUB2 indicated a differential reactivity towards ubiquitin based active-site probes carrying a vinyl-methylester, a 2-chloroethyl, or a 2-bromoethyl group at the C-terminus. Mutational analysis suggested that a narrow P1' site as observed in OTUB1 correlates with its ability to preferentially cleave lys^{48}- linked ubiquitin chains. Analysis of cellular interaction partners of OTUB1 by co-immunoprecipitation and tandem mass spectrometry experiments demonstrated that FUS (also known as TLS or CHOP) and Rack1 (also known as GNB2L1) are part of OTUB1 containing complexes, pointing towards a molecular function of this deubiquitylating enzyme in RNA processing and cell adhesion/morphology.

Introduction

Ubiquitin (Ub) is central for many biological processes including protein turnover, protein targeting, signal transduction, and regulation of transcription, and has been implicated in tumorigenesis, neurodegeneration and microbial pathogenesis. The relevance of Ub in these biological processes is reflected by the fact that several hundred genes have so far been linked to Ub conjugation and de-conjugation. Primary examples are the E3 ligases and deubiquitylating enzymes (DUBs), the former consisting of approximately 600 genes that are classified into the RING and HECT domain families [1], and the latter are classified into six main families, such as ubiquitin processing proteases (UBPs), ubiquitin C-terminal hydrolases (UCHs), Ataxin3/Josephin domains, ovarian tumor domain containing proteases (OTUs), pathogen encoded Ub processing proteases and JAMM proteases [2]. The OTU-family has recently attracted attention due the presence of conserved sequences found in viruses, bacteria, plants, yeast, and humans, and its role in immunity and viral infection [3]. It consists of a ca. 130 amino acid papain fold with a catalytic triad that is typically found in cysteine proteases [4]. Otubain 1 (OTUB1) and otubain 2 (OTUB2) are close homologues expressed in mammals [5]. Although ubiquitously expressed, OTUB1 is implicated in anergy induction in $CD4^+$ T lymphocytes, affecting the stability of the lymphocyte-specific E3 ligase GRAIL (Gene related to anergy in lymphocytes) [6]. Its immune-related functions were partially ascribed to specific splice variants, including ARF-1, found only in these cells [7]. In addition, OTUB1 binds the *Yersinia* pathogen encoded virulence factor YpkA [8]. Exemplified by A20 [9, 10], OTUB1 also likely acts upon a discrete set of substrates in contrast to Cezanne, which was shown to be a more general DUB [11]. Structural insights obtained for some of the OTU domain containing proteins, such as A20 [12, 13], OTUB2 [14] and yeast OTU1 in complex with a ubiquitin-Br3 derivative [15] confirm that the OTU domain encodes a rudimentary papain-like domain with considerable variations that may reflect functional diversity.

Here we present the crystal structure of human OTUB1 and show significant differences when compared with OTUB2. In addition to being selective towards Ub and to some extent NEDD8, but not ISG15 and SUMO1/2/3, OTUB1 prefers cleavage of lys^{48}-linked Ub as compared to lys^{63}-linked Ub chains, which is probably attributable to a narrow cavity at the P1' site. Mass spectrometric identification of cellular interaction partners suggests that OTUB1 may be generally involved in RNA processing and cell adhesion/morphology.

Results

Overall Structure

OTUB1 is an OTU family member with a conserved ovarian tumor domain between residues 85-271. Removal of the N-terminal sequence allowed OTUB1 (residues 40-271) to readily crystallize and diffract to 1.7 Å resolution. A molecular replacement strategy using coordinates from the OTUB2 structure was employed to determine the OTUB1 structure, revealing all residues in the construct except for the first five and asp^{238} in the β3-β4 loop. As with other papain-like proteases, the active site is formed at the interface of an α-helical lobe (α3-α10) and a β-sheet lobe (β1-β5), centered on the catalytic cysteine (cys^{91}), which is situated at the C-terminal pole of the α3 helix (Figure 1A, left panel). The P-side of the active site runs along one side of the interface, and the P'-side runs along the opposing side (Figure 1A and C). Interestingly, the conformation of the catalytic triad histidine (his^{265}) and its distance from the catalytic cysteine (cys^{91}, 5.5 Å) and catalytic aspartate (asp^{267}, 4.6 Å) is incompatible with catalysis (Figure 1B, top panel). Instead, his^{265} is sandwiched between the guanidinium and prolyl side chains of arg^{262} and pro^{87}, respectively, interacting with the catalytic asp^{267} through a pair of water molecules. In addition, the catalytic cysteine cys^{91} is tied-up through hydrogen bonds with the backbone carbonyl oxygen of arg^{86} and a water molecule that also interacts with glu^{214}. The conserved glutamic acid (glu^{214}) from the α9-α10 loop is inserted into the P1 pocket, forming hydrogen bonds with the C-terminal pole of the α3 helix and the backbone of the catalytic residue cys^{91}, thereby blocking access to the active site (Figure 1B, top panel). This unique structure corresponds to a non-productive conformation of the catalytic center not observed in any other cysteine proteases (Figure 1B). Our structure of the ligand-free OTUB1 might therefore represent an autoinhibited state, which likely is involved in a ligand-dependent induced fit mechanism.

Structural comparison of OTUB1 and OTUB2

Despite being highly homologous with OTUB2 (RMS value of 1.68, Figure 1 and [14]), OTUB1 displays a number of different structural features (Figure 1C and D), particularly in the vicinity of the catalytic triad and the P1/P1' pockets. Importantly, in contrast to OTUB1, the structure of OTUB2 reveals a more canonical active site, where the catalytic histidine (his^{224}) is within hydrogen-bonding distance of the catalytic cysteine and the pKa of his^{224} is enhanced by hydrogen bonds with the side chains of adjacent residues, including those of asn^{226} and thr^{45} [14] (Figure 1B, middle panel). But, unlike OTUB1, the P1/P2 pocket of OTUB2 is somewhat encumbered by the presence of ser^{223} from the β3-β4 loop. Differences in the OTUB1 β4-β5 and OTUB2 β3-β4 loop suggest that it may undergo conformational changes upon ubiquitin binding that then allow rearrangement of his^{265} for catalytic cysteine activation.

The P'-side of OTUB1, where the leaving lysyl group from a target substrate or ubiquityl group from a chained-substrate would be expected to bind, is significantly different from OTUB2. In addition to a dissimilar surface charge property in this region, the α2 helix of OTUB2 is kinked, a feature that is not observed in the OTUB1 structure (Figure 1C). An additional structural restriction of the catalytic cleft in OTUB1 is the presence of pro^{87} that is located in proximity to cys ^{91} (Figure 1B). In the OTUB2 structure this position is occupied by gly^{47}. The presence of a more bulky side chain could potentially contribute to OTUB1's cleavage preference for isopeptide bonds over ubiquitin C-terminal fusions, a trait that is not observed for OTUB2 [14].

A similar argument was made for explaining the specificity of the SUMO-specific protease SENP2 towards lysine deconjugation [16].

Structural comparison of OTUB1 and OTUB2 with yeast OTU1 bound to ubiquitin indicates conformational changes upon ligand binding

Yeast OTU1 has been recently crystallized in a covalent complex with a ubiquitin C-terminal Br3 derivative [15]. Although there is minimal primary sequence homology between the OTU domains of yeast OTU1 and human OTUB1 (< 15% identity), they share similar structural features, and a comparison may provide interesting insights into the conformational changes that occur upon ubiquitin binding (Figure 1 A and B). In addition to the ubiquitin tail, which makes typical residue-specific peptide interactions with the active site (classical P1-P4 substrate residues and the corresponding S1-S4 protease pockets), one face of the core domain of ubiquitin is also recognized by OTU1. This area of the enzyme, herein referred to as the SD site (the subsite of the enzyme that docks with the core globular domain of ubiquitin (residues 1-70)), mediates numerous interactions, including those centered on His^{192} and Ile^{221}, and is likely to contribute to the induce-fit mechanism of the enzyme, the K_m of the ubiquityl substrate, or the K_d of the ubiquityl inhibitor. OTUB2 contains a discordant loop (198-210) that would likely clash with ubiquitin binding. This region of OTUB1 forms a well-defined β-strand (β4), extending the β-sheet lobe, but not interfering with the putative ubiquitin binding region (Figure 1C). The flexible nature of a single residue in the β3-β4 loop (arg^{238}) in OTUB1 hints at the possibility that OTUB1 might adopt a conformation similar to that of OTUB2 during a regulatory cycle, and that the OTUB1 and OTUB2 structures may represent two conformational states in a regulatory pathway. Alternatively, these structural differences may suggest diverse ubiquitin binding modes.

Differential proteolytic fine specificities between OTUB1 and OTUB2

To profile potential differences in substrate specificity between OTUB1 and OTUB2, we subjected these enzymes to reaction with various ubiquitin-based active site probes that have subtle differences in their reactive electrophiles. Probes with a C-terminal 2-chloroethyl (Cl2), 2-bromoethyl (Br2), or vinyl methylester (VME) groups were incubated with enzyme and analyzed by electrophoresis and immunoblotting (Figure 2). OTUB2 reacted with all three probes equally well, whereas OTUB1 reacted with the alkyl halides, but not the vinyl methylester probe (Figure 2B and C). These results hint that OTUB1 and OTUB2 may have slightly different specificities, likely expressed by structural differences proximal to their catalytic centers. Furthermore, this supports the notion that OTUB1 is autoinhibited and that specific substrates, or interactors, are required for its activation, likely through an induced fit mechanism.

OTUB1 specificity towards ubiquitin and Ubls

In order to test the deubiquitylation properties of OTUB1, we examined its ability to cleave linear di-ubiquitin as well as lys^{48}- and lys^{63}-linked tetra-ubiquitin by immunoblotting and mass spectrometry. OTUB1 did not cleave di-ubiquitin, consistent with previous observations (Figure 3A, [5]). At an enzyme to substrate ratio of 1:5, OTUB1 clearly showed a preference for cleaving lys^{48}-linked tetra-ubiquitin when assessed by anti-ubiquitin immunoblotting (Figure 3B). This preference was confirmed by mass spectrometry-based analysis (Figure 3C). The use of a higher enzyme to substrate ratio (1:1.5) in the latter analysis further indicated that OTUB1 may also slowly cleave lys^{63}-linked ubiquitin chains (Figure 3C). Ubiquitin cleavage assays

performed with a truncated form of OTUB1 lacking the first 40 amino acids did not affect the proteolytic properties of OTUB1 (data not shown), indicating that the N-terminal region of OTUB1 does not influence cleavage preference *in vitro*.

We further examined the ability of OTUB1 to catalyze general deubiquitylation reactions by examining crude extracts prepared from HEK293T cells over-expressing either wildtype or C91S inactive mutant OTUB1. We observed only minor effects on the level of poly-ubiquitylated material *in vitro* and in living cells (Figure 3D). This observation is consistent with previous findings [5, 6] and suggests that OTUB1 may act only on a discrete set of substrates.

In contrast to OTUB1, OTUB2 appears to readily cleave lys^{63}- over lys^{48}-linked tetra-ubiquitin (Figure 4A). We therefore evaluated structural differences between OTUB1 and OTUB2 that might explain their differential reactivity towards the active site probe Ub-VME and the different Ub chains. In particular, we noted that the P1' site of OTUB1 was sterically restricted by the presence of a proline residue at position 87, which in the corresponding position in the OTUB2 structure is a glycine (G47) (Figure 1B). OTUB1 P87G and OTUB2 G47P mutant proteins were therefore generated and tested for their ability to cleave different Ub chains. Interestingly, we observed that the steric restriction imposed by a proline residue in this area of the P1' site in OTUB2 affected the ability of cleaving lys^{63}-linked tetra-ubiquitin, whereas cleavage slightly improved upon the introduction of a glycine residue at this position in OTUB1 (Figure 4A). Consistent with this, we observed that cleavage of Ub-AMC was also altered, although to a greater extent by the G47P mutation in OTUB2 as compared to the inverse modification in OTUB1 (Figure B). Combined, these results support the notion that OTUB1 has a more restricted specificity, mainly towards lys^{48}-linked Ub chains, due to a narrower P1' site, and that OTUB1 and OTUB2 may act on a different set of substrates although the overall structure of these enzymes is similar.

We next examined the possibility that OTUB1 recognizes other ubiquitin-like modifiers. For this purpose, an N-terminally biotinylated seven amino acid peptide was conjugated to either ubiquitin, NEDD8, ISG15 or SUMO1 in order to create substrates with an isopeptide bond. These were incubated with either OTUB1 or a positive control (Figure 5A). Our results indicate that OTUB1 has a clear preference for ubiquitin and at a slower rate for NEDD8 conjugates. In addition, OTUB1 was unable to cleave di-SUMO2 and di-SUMO3 substrates (Figure 5B). Since these experiments are based on the use of a mono- or di-Ub/Ubl based substrate, the specificity may be different for poly Ub/Ubls, in particular in living cells where OTUB1 may be present in multi-protein complexes in which co-factors could influence its cleavage specificity.

Initial analysis of intracellular OTUB1 interacting proteins

As shown previously, OTUB1 was found to be in complex with GRAIL and USP8 in lymphocytes [6] and can interact with the enteropathogen *Yersinia* encoded virulence factor YpkA (YopO) [8]. In order to identify potential OTUB1 interacting proteins in a non-hematopoietic context, we performed proteomics-based studies using co-immunoprecipitation and identification by tandem mass spectrometry. HEK293T cells were transiently transfected with either wildtype or catalytically inactive (C91S) HA-TEV-SBP tagged OTUB1 (HA: hemagglutinin, TEV: Tobacco Etch Virus, SBP: streptavidin binding peptide). The inactive mutant was used as a "substrate trap", preventing potential substrates from being turned over and

released [17]. Cell extracts were prepared after 24 hours either with or without detergent solubilization and subjected to anti-HA immunoprecipitation, followed by cleavage of bound material using Tobacco Etch Virus (TEV) protease. This approach was previously used to reduce background due to non-specific protein binding to beads [18]. Analysis by gel electrophoresis and silver staining revealed a total of >80 proteins, from which 26 were uniquely present when HA-OTUB1 was expressed, but not detected when HA-OTUB1 was absent (Figure 6 and Supplementary Table 1). The catalytically inactive OTUB1 mutant (C91S) showed a slightly faster migration profile, a feature commonly observed with mutant proteins. We also detected OTUB1 material that was of higher molecular weight, indicating the presence of posttranslational modifications.

Among the hits, two proteins, FUS/TLS and Rack1 were further evaluated with specific pull-down and follow-up biochemical experiments. Immunoprecipitation of HA-OTUB1 followed by anti FUS/TLS and anti Rack1 immunoblotting confirmed their presence in OTUB1 complexes, but not in controls (Figure 7A). Since FUS/TLS can exist in different forms [19] and also as fusion proteins in the context of oncogenic transformations [20, 21], we examined the effect of OTUB1 on FUS/TLS stability by size-exclusion chromatography and immunoblotting using an anti-FUS polyclonal antibody that detects multiple molecular weight forms of this protein (Figure 7B, left panel). FUS/TLS appeared predominantly as high molecular weight species, but upon over-expression of OTUB1, a FUS/TLS polypeptide of the expected molecular weight of ~60kDa was detected (Figure 7B, left panel). Using a monoclonal antibody that recognizes a C-terminal epitope of FUS/TLS, we observed a similar ~60kDa form that appears to be stabilized upon over-expression of OTUB1, but not in the presence of the mutant C91S (Figure 7B, right panel). We noted that only a small fraction of high molecular weight FUS/TLS was affected by OTUB1, and therefore examined the extent of poly-ubiquitylated FUS/TLS present in cells. Transfection experiments with HA-tagged ubiquitin, subsequent anti-HA immunoprecipitation and anti-FUS immunoblotting indicated that a small fraction of FUS is indeed ubiquitylated (Figure 7C). Combined, these data suggest that the catalytic activity of OTUB1 may affect the ubiquitylation state of a small subset of FUS/TLS protein.

Discussion

The structure of OTUB1 reveals a number of properties that address activation and substrate specificity. In analogy to auto-inhibition observed in HAUSP, USP8, and USP14 [22-24], where the unliganded active site is blocked by surface loops, the apo form of OTUB1 adopts a conformation of the active site that appears closed and not competent for catalysis. A comparison between OTUB1 and the yeast OTU1-UbBr3 structure further suggests that a conformational change would activate their respective catalytic triad (Figure 1 and [15]). We propose that the tight OTUB1 β4-β5 loop immediately prior to his^{265} (RPG^{264}) and the α9-α10 loop, which influences the catalytic cysteine through glu^{214}, could play a role by mediating a conformational change upon ubiquitin binding, allowing his^{265} to participate in the catalytic triad. However, analysis of the geometry of the active sites revealed subtle variations between OTUB1 and OTUB2, which were reflected by a differential reactivity with alkyl halide and vinyl methyl ester based ubiquitin probes (Figure 2 and [25]), but also Ub-AMC (Figure 4B). This may be explained by subtle structural differences between the P1' sides of those enzymes. In particular, steric hindrance by the presence of pro^{87} in OTUB1's catalytic center may prevent the accommodation of the AMC fluorescent group and the vinyl methylester side chain of the probe, whereas the alkyl halides are able to react with the catalytic cysteine to undergo a nucleophilic substitution reaction. Consistent with this notion, the OTUB2 structure contains gly^{47} at this position (Figure 1). Mutational analysis using recombinant OTUB1 P87G and OTUB2 G47P mutants confirmed that steric hindrance at this position compromises the ability to cleave Ub-AMC and to react with the probes, but substitution of pro^{87} with a glycine in OTUB1 did not improve Ub-AMC cleavage, nor did it restore reactivity towards the Ub-VME probe (Figure 4B and data not shown). This suggests that other structural constrains must exist, or that the introduction of a mutation in this position may also lead to more complex rearrangements of the P1' site. Reactivity of OTUB1 towards the Ub-2-chloroethyl probe was observed in our experiments here, but was not detected in a previous study [25]. This might be due to over-expression of OTUB1 in the labeling assay (Figure 2B and C), whereas at physiological levels other DUBs present in cell extracts may effectively compete for binding to the Ub-chloride probe. Different structural features and discrepancies in the reactivity towards the active site Ub probes between OTUB1 and OTUB2 may hint towards a divergence in their cleavage or substrate specificities. This hypothesis was confirmed by the finding that OTUB1 has a preference for cleaving lys^{48}- over lys^{63}-linked tetra-ubiquitin, whereas the opposite appears to be the case for OTUB2. We observed that full-length OTUB2 retained cleavage activity which was unchanged when deleting the C-terminal amino acids 229-234 as compared to a previous study ([5] and unpublished data). Modification of the P1' site in OTUB1 by a P87G and in OTUB2 by a G47P substitution affected the ability of these enzymes to cleave lys^{63}-linked tetra-ubiquitin in the opposite way (Figure 4). This result is fairly surprising, since lys^{63}-linked polyubiquitin chains are in an extended conformation as compared to lys^{48}-linke chains, and therefore would be expected to be less susceptible to structural constrains in the P1' pocket [26]. Recent structural information as well as predictions suggest that the P1' site harbors the isopeptide bond lysine side chain, and that the nature of the binding pocket for distal ubiquitin is partially responsible for the affinity towards different Ub chains [27]. Our results provide insights into the role of non-catalytic side chains that can influence proteolysis of different ubiquitin chains. However, other structural elements such as a kinked α2 helix present in OTUB2, but not OTUB1, may be necessary to determine linkage preference.

The oxyanion hole in OTUB1 appears to be formed by the backbone amide of the catalytic cys[91] and the backbone amide of asp[88]. This is very similar to the oxyanion hole geometry observed in OTUB2, A20 and yeast OTU1, thereby confirming that this may be an element specifically observed in OTUs, but not other cysteine protease families [12, 14, 15].

With the exception of virus encoded OTU variants that have acquired an additional specificity for ISG15 [3], ovarian tumor domain containing deubiquitylating enzymes have a preference for ubiquityl derivatives. Our data confirm this finding and further indicates that OTUB1 may have some reactivity towards NEDD8. This apparent dual specificity has also been observed for other DUBs, such as UCH-L1, UCH-L3 [28, 29], USP21 and the COP9 signalosome [30, 31]. As observed with the OTU domains of A20 and yeast OTU1, OTUB1 has a preference for lys[48]- over lys[63]- linked polyubiquitin (Figure 3 and [15]), whereas OTUB2 prefers the latter (Figure 4). However, as observed for A20, the *in vitro* result may not necessarily reflect biological behavior in living cells, a trait that remains to be examined for OTUB1 specific substrates.

As a step towards addressing this issue, proteomics and mass spectrometry based screens for OTUB1 interactors and substrates identified a number of candidates (Supplementary Table 1). We noted a considerable amount of co-immunoprecipitating nuclear proteins, such as cell growth nucleolar proteins, DNA topoisomerases and several RNA helicases sharing a DEAD box motif (Figure 6, Supplementary Table 1). OTUB1 does contain a predicted nuclear localization sequence NLS (residues 69-85), and initial microscopy studies suggest that OTUB1 subsets are present in the nucleus ([32] and unpublished data). On the other hand, RNA binding proteins are abundant and commonly found as contaminants in mass spectrometry based pull-down assays [25], although all proteins listed were not detectable in controls without the bait protein (Figure 6). Among the hits, FUS/TLS and Rack1 were validated by co-immunoprecipitation experiments. FUS/TLS has been described as an RNA splicing factor involved in chromosomal aberrations observed in Ewing tumors, erythroleukemia, acute myelocytic/lymphoblastic leukemia and fibrosarcoma [33-35], and it was shown to be present in protein networks containing CIP29 and DDX39 [36]. The major form of ~60kDa can be recognized with an anti-FUS/TLS monoclonal antibody ([37] and Figure 7A and B). Additional high-molecular weight forms can also be detected using a polyclonal anti-FUS/TLS antibody (Figure 7B). OTUB1, when over-expressed in HEK293T cells, has an effect on the molecular size of a subset of FUS/TLS containing material (Figure 7B). This appears to be dependent on the catalytic activity of OTUB1, suggesting that a functional OTUB1 enzyme is required for this process. By co-transfection experiments with HA-tagged ubiquitin, we were able to observe that a small fraction of the FUS/TLS containing high molecular weight material is ubiquitylated (Figure 7C). Alteration of a small subset did not lead to any significant changes in total FUS/TLS protein levels, although the 60kDa form of FUS/TLS appears to be present in more chromatography fractions when wildtype OTUB1 was over-expressed (Fig 7B, left and right panels). Attempts to address whether FUS/TLS may be a direct substrate of OTUB1 turned out to be challenging, in part due to the fact that FUS/TLS may exist in multiple forms, and that a major fraction of high molecular weight material reactive to polyclonal anti-FUS antibody is not ubiquitylated [38]. OTUB1 may act as a deubiquitylating enzyme in this case, or could function as a scaffold protein to mediate activity of another deubiquitylating enzyme, such as USP8 [6], although its effect on FUS appears to be dependent on intact enzymatic activity (Figure 7B). FUS/TLS as well as

Rack1 were also suggested to play a role in the initiation of cell spreading by modulating the formation of spreading initiation centers (SIC) [39]. Taken together, our results suggest that OTUB1 may be linked to these biological processes, and provide the framework for more detailed studies on the functional contribution of OTUB1 within these pathways.

Materials and Methods

Cell lines, reagents and antibodies

Chemicals were purchased from Sigma-Aldrich, UK, unless indicated otherwise. The cDNA for human OTUB1 was obtained by performing a PCR reaction with a spleen cDNA library (Invitrogen, CA, USA) as a template with the following primers: 5'-3' CTA CTA GCT AGC ATG GCG GCG GAG GAA CC and 3'-5' CGG CGG CTC GAG CTA TTT GTA GAG GAT ATC GTA G. The primers included a 5' NheI and a 3'XhoI site for directional cloning into a pcDNA3.1 vector containing a C-terminal SBP-TEV-HA tag. The OTUB1-$_{HA}$ C91S mutant was created using the QuikChange II Site Directed Mutagenesis kit by Stratagene (USA). OTUB1-$_{SBP\text{-}TEV\text{-}HA}$ (OTUB1-$_{HA}$) wildtype and mutant were sub-cloned into the bicystronic pEF-IRES vector [40] kindly provided by Dr. Marek Cebecauer (Imperial College, London, UK) using the 5' NheI and 3' Xba I restriction sites. Residues 40–271 were subcloned into pET28a-LIC for structural studies. The cDNA for human OTUB2 was obtained by performing a PCR reaction with a spleen cDNA library (Invitrogen, CA, USA) as a template with the following primers: 5'-3' CTA CTA GCT AGC ATG AGT GAA ACA TCT TTC AAC C and 3'-5' CGG CGG CTC GAG TCA ATG TTT ATC GGC TGC ATA AAG G. The primers contained a 5' NheI and a 3'XhoI site for directional cloning into a pcDNA3.1 vector containing a C-terminal SBP-TEV-HA tag as well as a pET28aLIC vector (Invitrogen) for bacterial expression. The proteasome inhibitor ZL_3VS was kindly provided by Dr. Herman Overkleeft (Leiden University, The Netherlands). The antibodies used in this study are described in Supplementary Material & Methods.

Protein purification, crystallization, and structure determination

OTUB1(40–271) was expressed in *E. coli* BL21 (DE3) and grown in Terrific Broth (TB) in the presence of 50µg/mL kanamycin at 37ºC to an OD_{600} of 0.5. Cells were induced overnight at 15ºC with 0.05mM isopropyl-1-thio-D-galactopyranoside (IPTG). The expressed protein was purified from cell pellets using a TALON metal-affinity resin column (BD Biosciences) at 4ºC, cleaved with thrombin (Sigma T9681), and purified by gel filtration on a HighLoad 16/60 Superdex 200 column (GE Healthcare, Amersham). Purified protein (68mg/mL) was crystallized at room temperature using the hanging drop vapor diffusion method when mixed with an equal volume of the reservoir solution (30% PEG 8000, 0.2 M Sodium acetate, and 0.1 M Sodium cacodylate at pH 6.5). Crystals were cryoprotected in a 50:50 mixture of Paratone-N and mineral oil and frozen in liquid nitrogen. Diffraction data was obtained using an FR-E generator and RAXIS IV++ detector and processed with HKL2000 [41]. A molecular replacement solution using OTUB2 (PDB code 1TFF) was found with the program MolRep [42]. The refinement procedures were carried out with REFMAC5 [43]. Model fitting to electron density maps was performed manually using Coot [44]. Final refinement statistics are summarized in Table 1. The

generation of recombinant wildtype and mutant OTUB1 / P87G and OTB2 G47P protein is described in detail in Supplementary Materials & Methods.

Preparation of ubiquitin and UBl substrates and isopeptidase assays
The synthesis and preparation of ubiquitin and ubiquitin-like protein based on the Ub/Ubl-orthogonal peptide scaffold containing an N-terminal biotin moiety was performed essentially as described [45]. Further details are reported in Supplementary Materials & Methods.

Preparation of ubiquitin-specific active site probes and activity-based profiling assays
The synthesis and preparation of HA-tagged Ubiquitin active-site probes containing a C-terminal 2-bromoethyl, 2-chloroethyl and vinyl methylester group was performed essentially as reported previously [25]. Further details are described in Supplementary Materials & Methods.

Linear di-ubiquitin, lys^{48}-/lys^{63}-linked tetra-ubiquitin, di-SUMO and Ub-AMC cleavage assays
Linear di-ubiquitin, lys^{48}-, lys^{63}-linked tetra-ubiquitin, di-SUMO2, di-SUMO3, Ub-AMC, UCH-L3 and SENP2 were purchased from Boston Biochem (USA). A 20 µl solution containing reaction buffer (50mM Tris pH 7.4, 2mM DTT), linear di-ubiquitin, lys^{48}-, lys^{63} tetra-ubiquitin, di-SUMO2 or di-SUMO3 (250nM final concentration) was incubated with recombinant OTUB1 or OTUB2 proteins (50nM final concentration) or 5µg cell extract (prepared as described below) in a final reaction mix volume of 20µl for the indicated times at 37^{o}C. The reactions were stopped by adding reducing SDS sample buffer, followed by separation on Tris-Tricine SDS-PAGE [46] and visualization by anti-ubiquitin or anti-SUMO immunoblotting. For the analysis by mass spectrometry, 1.5µg lys^{48}- or lys^{63} tetra-ubiquitin was incubated with 1µg recombinant OTUB1 for the indicated times and subjected to analysis by infusion electrospray MS (LC/MSD-TOF, Agilent 1100 series). Ub-AMC cleavage assays were performed essentially as reported [45] and further details described in Supplementary Methods.

Identification of OTUB1 interactors by tandem mass spectrometry
HEK293T cells were grown to confluence in DMEM medium containing 10% Fetal Bovine Serum (FBS) and streptomycin/penicillin. Cells were then transferred to 150mm, 100mm, 50mm or 6-well tissue culture dishes at a concentration of 0.4x10^{6}/ml and grown overnight at 37^{o}C. The cells were then washed and the transfection was performed using SuperFect reagent (Qiagen, UK), according to the manufacturer's protocol, followed by incubation overnight at 37^{o}C. ~1x10^{9} cells per sample were lysed using glass beads (Sigma) in 150mM NaCl, 5mM $CaCl_2$, 50mM Tris pH 7.4, 250mM sucrose containing protease inhibitor cocktail (Roche Applied Science, USA) as described [25]. Alternatively, cells were lysed in 0.1% NP-40, 150mM NaCl, 20mM $CaCl_2$, 50mM Tris pH 7.4. For immunoprecipitation protein lysates (5mg per sample) were first diluted in NET buffer (50mM Tris, 5mM EDTA, 150mM NaCl, 0.5% NP-40, pH 7.4) to a protein concentration of 1mg/ml, and pre-cleared with agarose-coupled Protein A beads (Sigma-Aldrich, UK) for one hour at 4^{o}C. Immunoprecipitation was then carried out either for two hours or overnight at 4^{o}C. Material was eluted from the beads using the tobacco etch virus protease (TEV, Invitrogen) for two hours at 4^{o}C and separated by SDS-PAGE and visualized using silver staining. Gel bands that were unique to lanes containing OTUB1 as well as the corresponding areas in the control lane were excised and subjected to in-gel digestion with trypsin and analysis by nano-LC-MS/MS tandem mass spectrometry as described [47].

Gel filtration and immunoblotting
Fractionation of crude cell extracts prepared from HEK293T cells expressing control vector, wildtype or C91S mutant OTUB1 was performed using size exclusion chromatography with an HPLC system (Agilent HP1200, Karlsruhe, Germany). Sample protein concentration was determined using a Lowry assay (Bio-Rad, UK). 300µl (2.5mg/ml) was loaded and separation achieved using a Zorbax G450 gel filtration column (9.6mm x 250mm, Agilent, Karlsruhe, Germany) at a flow rate of 0.7ml/min in lysis buffer (0.5% NP-40, 150mM NaCl, 5mM $CaCl_2$, 50mM Tris pH 7.4). Fractions of 0.5ml or 0.7ml were collected, protein material was precipitated using chloroform/methanol [48], followed by SDS-PAGE based separation and immunoblotting using anti-FUS/TLS (Santa Crux, USA) or anti-OTUB1 antibodies.

Molecular graphics
All structural figures were grenerated by PyMOL v.99vc6 [49].

Acknowledgements
We are indebted to Dr. Mark Cebecauer (Imperial College London, UK) for providing us with the pEF-IRES expression constructs. We also thank Dr. Herman Overkleeft (Leiden University, The Netherlands) for the general gift of proteasome inhibitors, Dr. Nicola Ternette for expert assistance with the generation of constructs and Dr. Norma Masson for the HA-ubiquitin construct. The Structural Genomics Consortium is a registered charity (number 1097737) that receives funds from the Canadian Institutes for Health Research, the Canadian Foundation for Innovation, Genome Canada through the Ontario Genomics Institute, GlaxoSmithKline, Karolinska Institutet, the Knut and Alice Wallenberg Foundation, the Ontario Innovation Trust, the Ontario Ministry for Research and Innovation, Merck & Co., Inc., the Novartis Research Foundation, the Swedish Agency for Innovation Systems, the Swedish Foundation for Strategic Research and the Wellcome Trust. We also thank Drs. Kerry.R. Love and Hidde.L. Ploegh (Whitehead Institute, MIT, Boston, USA) for providing us with the pTYB2 plasmid. B.M.K. is supported by a MRC New Investigation Award. M.A. is supported by the Swedish Brain Foundation, the Loo and Hans Ostermans Foundation for geriatric research and the Foundation for Geriatric Diseases at the Karolinska Institutet, Sweden. We also wish to acknowledge the Computational Biology Research Group at the University of Oxford for use of their services in this project.

Table1: Data collection and refinement statistics

Data collection statistics	
Crystal	Human Otubain 1 (residues 40–271)
Space group	*C* 2
Unit-cell parameters (Å, °)	a= 81.25, b= 50.89, c= 54.72, β = 101.96
Wavelength (Å)	1.54178
Resolution (Å)[a]	29.15 - 1.69
Total reflections	23651
Unique reflections	7629
Completeness (%)[a]	97.2 (80.8)
R_{merge} (%)[a]	7.3 (39.0)
I/σ(I) [a]	18.7 (1.9)
Refinement statistics	
Resolution range (Å)	53.53-1.69
No. of reflections	22222
No. of non-hydrogen atoms	
Protein	1882
Water	124
Rwork (%)	19.5
Rfree (%)	23.9
R.m.s. deviations	
Bond length (Å)	0.016
Bond angle (°)	1.435
Average B-factors (Å^2)	
Otubain 1	29.4
Water	37.5

[a] Values in parentheses are for the highest resolution shell. PDB code: 2ZFY.

References

Reference list

1 Li, W. and Ye, Y. (2008) Polyubiquitin chains: functions, structures, and mechanisms. Cell Mol Life Sci

2 Nijman, S. M., Luna-Vargas, M. P., Velds, A., Brummelkamp, T. R., Dirac, A. M., Sixma, T. K. and Bernards, R. (2005) A genomic and functional inventory of deubiquitinating enzymes. Cell. **123**, 773-786

3 Frias-Staheli, N., Giannakopoulos, N. V., Kikkert, M., Taylor, S. L., Bridgen, A., Paragas, J., Richt, J. A., Rowland, R. R., Schmaljohn, C. S., Lenschow, D. J., Snijder, E. J., Garcia-Sastre, A. and Virgin, H. W. t. (2007) Ovarian tumor domain-containing viral proteases evade ubiquitin- and ISG15-dependent innate immune responses. Cell Host Microbe. 2, 404-416

4 Makarova, K. S., Aravind, L. and Koonin, E. V. (2000) A novel superfamily of predicted cysteine proteases from eukaryotes, viruses and Chlamydia pneumoniae. Trends Biochem Sci. **25**, 50-52

5 Balakirev, M. Y., Tcherniuk, S. O., Jaquinod, M. and Chroboczek, J. (2003) Otubains: a new family of cysteine proteases in the ubiquitin pathway. EMBO Rep. **4**, 517-522

6 Soares, L., Seroogy, C., Skrenta, H., Anandasabapathy, N., Lovelace, P., Chung, C. D., Engleman, E. and Fathman, C. G. (2004) Two isoforms of otubain 1 regulate T cell anergy via GRAIL. Nat Immunol. **5**, 45-54

7 Fathman, C. G., Soares, L., Chan, S. M. and Utz, P. J. (2005) An array of possibilities for the study of autoimmunity. Nature. **435**, 605-611

8 Juris, S. J., Shah, K., Shokat, K., Dixon, J. E. and Vacratsis, P. O. (2006) Identification of otubain 1 as a novel substrate for the Yersinia protein kinase using chemical genetics and mass spectrometry. FEBS Lett. **580**, 179-183

9 Evans, P. C., Ovaa, H., Hamon, M., Kilshaw, P. J., Hamm, S., Bauer, S., Ploegh, H. L. and Smith, T. S. (2004) Zinc-finger protein A20, a regulator of inflammation and cell survival, has de-ubiquitinating activity. Biochem J. **378**, 727-734

10 Turer, E. E., Tavares, R. M., Mortier, E., Hitotsumatsu, O., Advincula, R., Lee, B., Shifrin, N., Malynn, B. A. and Ma, A. (2008) Homeostatic MyD88-dependent signals cause lethal inflamMation in the absence of A20. J Exp Med. **205**, 451-464

11 Evans, P. C., Smith, T. S., Lai, M. J., Williams, M. G., Burke, D. F., Heyninck, K., Kreike, M. M., Beyaert, R., Blundell, T. L. and Kilshaw, P. J. (2003) A novel type of deubiquitinating enzyme. J Biol Chem. **278**, 23180-23186

12 Komander, D. and Barford, D. (2008) Structure of the A20 OTU domain and mechanistic insights into deubiquitination. Biochem J. **409**, 77-85

13 Lin, S. C., Chung, J. Y., Lamothe, B., Rajashankar, K., Lu, M., Lo, Y. C., Lam, A. Y., Darnay, B. G. and Wu, H. (2008) Molecular basis for the unique deubiquitinating activity of the NF-kappaB inhibitor A20. J Mol Biol. **376**, 526-540

14 Nanao, M. H., Tcherniuk, S. O., Chroboczek, J., Dideberg, O., Dessen, A. and Balakirev, M. Y. (2004) Crystal structure of human otubain 2. EMBO Rep. **5**, 783-788

15 Messick, T. E., Russell, N. S., Iwata, A. J., Sarachan, K. L., Shiekhattar, R., Shanks, J. R., Reyes-Turcu, F. E., Wilkinson, K. D. and Marmorstein, R. (2008) Structural basis for ubiquitin recognition by the otu1 ovarian tumor domain protein. J Biol Chem. **283**, 11038-11049

16 Reverter, D. and Lima, C. D. (2006) Structural basis for SENP2 protease interactions with SUMO precursors and conjugated substrates. Nat Struct Mol Biol. **13**, 1060-1068

17 Overall, C. M., Tam, E. M., Kappelhoff, R., Connor, A., Ewart, T., Morrison, C. J., Puente, X., Lopez-Otin, C. and Seth, A. (2004) Protease degradomics: mass spectrometry discovery of protease substrates and the CLIP-CHIP, a dedicated DNA microarray of all human proteases and inhibitors. Biol Chem. **385**, 493-504

18 Knuesel, M., Wan, Y., Xiao, Z., Holinger, E., Lowe, N., Wang, W. and Liu, X. (2003) Identification of novel protein-protein interactions using a versatile mammalian tandem affinity purification expression system. Mol Cell Proteomics. **2**, 1225-1233

19 Morohoshi, F., Arai, K., Takahashi, E. I., Tanigami, A. and Ohki, M. (1996) Cloning and mapping of a human RBP56 gene encoding a putative RNA binding protein similar to FUS/TLS and EWS proteins. Genomics. **38**, 51-57

20 Riggi, N. and Stamenkovic, I. (2007) The Biology of Ewing sarcoma. Cancer Lett. **254**, 1-10

21 Perez-Losada, J., Sanchez-Martin, M., Rodriguez-Garcia, M. A., Perez-Mancera, P. A., Pintado, B., Flores, T., Battaner, E. and Sanchez-Garcia, I. (2000) Liposarcoma initiated by FUS/TLS-CHOP: the FUS/TLS domain plays a critical role in the pathogenesis of liposarcoma. Oncogene. **19**, 6015-6022

22 Avvakumov, G. V., Walker, J. R., Xue, S., Finerty, P. J., Jr., Mackenzie, F., Newman, E. M. and Dhe-Paganon, S. (2006) Amino-terminal dimerization, NRDP1-rhodanese interaction, and inhibited catalytic domain conformation of the ubiquitin-specific protease 8 (USP8). J Biol Chem. **281**, 38061-38070

23 Hu, M., Li, P., Song, L., Jeffrey, P. D., Chenova, T. A., Wilkinson, K. D., Cohen, R. E. and Shi, Y. (2005) Structure and mechanisms of the proteasome-associated deubiquitinating enzyme USP14. EMBO J. **24**, 3747-3756

24 Hu, M., Li, P., Li, M., Li, W., Yao, T., Wu, J. W., Gu, W., Cohen, R. E. and Shi, Y. (2002) Crystal structure of a UBP-family deubiquitinating enzyme in isolation and in complex with ubiquitin aldehyde. Cell. **111**, 1041-1054

25 Borodovsky, A., Ovaa, H., Kolli, N., Gan-Erdene, T., Wilkinson, K. D., Ploegh, H. L. and Kessler, B. M. (2002) Chemistry-based functional proteomics reveals novel members of the deubiquitinating enzyme family. Chem Biol. **9**, 1149-1159

26 Balakirev, M. Y. and Wilkinson, K. D. (2008) OTU takes the chains OUT. Nat Chem Biol. **4**, 227-228

27 Sato, Y., Yoshikawa, A., Yamagata, A., Mimura, H., Yamashita, M., Ookata, K., Nureki, O., Iwai, K., Komada, M. and Fukai, S. (2008) Structural basis for specific cleavage of Lys 63-linked polyubiquitin chains. Nature. **455**, 358-362

28 Misaghi, S., Galardy, P. J., Meester, W. J., Ovaa, H., Ploegh, H. L. and Gaudet, R. (2005) Structure of the ubiquitin hydrolase UCH-L3 complexed with a suicide substrate. J Biol Chem. **280**, 1512-1520

29 Hemelaar, J., Borodovsky, A., Kessler, B. M., Reverter, D., Cook, J., Kolli, N., Gan-Erdene, T., Wilkinson, K. D., Gill, G., Lima, C. D., Ploegh, H. L. and Ovaa, H. (2004) Specific and covalent targeting of conjugating and deconjugating enzymes of ubiquitin-like proteins. Mol Cell Biol. **24**, 84-95

30 Wei, N. and Deng, X. W. (2003) The COP9 signalosome. Annu Rev Cell Dev Biol. **19**, 261-286

31 Gong, L., Kamitani, T., Millas, S. and Yeh, E. T. (2000) Identification of a novel isopeptidase with dual specificity for ubiquitin- and NEDD8-conjugated proteins. J Biol Chem. **275**, 14212-14216

32 Shan, T. L., Tang, Z. L., Guo, D. Z., Yang, S. L., Mu, Y. L., Ma, Y. H., Guan, W. J. and Li, K. (2008) Partial molecular cloning, characterization, and analysis of the subcellular localization and expression patterns of the porcine OTUB1 gene. Mol Biol Rep

33 Walsby, E. J., Gilkes, A. F., Tonks, A., Darley, R. L. and Mills, K. I. (2007) FUS expression alters the differentiation response to all-trans retinoic acid in NB4 and NB4R2 cells. Br J Haematol. **139**, 94-97

34 Shing, D. C., McMullan, D. J., Roberts, P., Smith, K., Chin, S. F., Nicholson, J., Tillman, R. M., Ramani, P., Cullinane, C. and Coleman, N. (2003) FUS/ERG gene fusions in Ewing's tumors. Cancer Res. **63**, 4568-4576

35 Perrotti, D., Bonatti, S., Trotta, R., Martinez, R., Skorski, T., Salomoni, P., Grassilli, E., Lozzo, R. V., Cooper, D. R. and Calabretta, B. (1998) TLS/FUS, a pro-oncogene involved in multiple chromosomal translocations, is a novel regulator of BCR/ABL-mediated leukemogenesis. EMBO J. **17**, 4442-4455

36 Sugiura, T., Sakurai, K. and Nagano, Y. (2007) Intracellular characterization of DDX39, a novel growth-associated RNA helicase. Exp Cell Res. **313**, 782-790

37 Riggi, N., Cironi, L., Provero, P., Suva, M. L., Stehle, J. C., Baumer, K., Guillou, L. and Stamenkovic, I. (2006) Expression of the FUS-CHOP fusion protein in primary mesenchymal progenitor cells gives rise to a model of myxoid liposarcoma. Cancer Res. **66**, 7016-7023

38 Perrotti, D., Iervolino, A., Cesi, V., Cirinna, M., Lombardini, S., Grassilli, E., Bonatti, S., Claudio, P. P. and Calabretta, B. (2000) BCR-ABL prevents c-jun-mediated and proteasome-dependent FUS (TLS) proteolysis through a protein kinase CbetaII-dependent pathway. Mol Cell Biol. **20**, 6159-6169

39 de Hoog, C. L., Foster, L. J. and Mann, M. (2004) RNA and RNA binding proteins participate in early stages of cell spreading through spreading initiation centers. Cell. **117**, 649-662

40 Hobbs, S., Jitrapakdee, S. and Wallace, J. C. (1998) Development of a bicistronic vector driven by the human polypeptide chain elongation factor 1alpha promoter for creation of stable mammalian cell lines that express very high levels of recombinant proteins. Biochem Biophys Res Commun. **252**, 368-372

41 Otwinowski, Z. and Minor, W. (1997) Diffraction Data Collected in Oscillation Mode, part A. Methods in Enzymology. **276**, 307-326

42 Vagin, A. and Teplyakov, A. (1997) MOLREP: an automated program for molecular replacement. Journal of Applied Crystallography. **30**, 1022-1025

43 Murshudov, G. N., Vagin, A. A. and Dodson, E. J. (1997) Refinement of macromolecular structures by the maximum-likelihood method. Acta Crystallogr D Biol Crystallogr. **53**, 240-255

44 Emsley, P. and Cowtan, K. (2004) Coot: model-building tools for molecular graphics. Acta Crystallogr D Biol Crystallogr. **60**, 2126-2132

45 Kattenhorn, L. M., Korbel, G. A., Kessler, B. M., Spooner, E. and Ploegh, H. L. (2005) A deubiquitinating enzyme encoded by HSV-1 belongs to a family of cysteine proteases that is conserved across the family Herpesviridae. Mol Cell. **19**, 547-557

46 Schagger, H. and von Jagow, G. (1987) Tricine-sodium dodecyl sulfate-polyacrylamide gel electrophoresis for the separation of proteins in the range from 1 to 100 kDa. Anal Biochem. **166**, 368-379

47 Batycka, M., Inglis, N. F., Cook, K., Adam, A., Fraser-Pitt, D., Smith, D. G., Main, L., Lubben, A. and Kessler, B. M. (2006) Ultra-fast tandem mass spectrometry scanning combined with monolithic column liquid chromatography increases throughput in proteomic analysis. Rapid Commun Mass Spectrom. **20**, 2074-2080

48 Wessel, D. and Flugge, U. I. (1984) A method for the quantitative recovery of protein in dilute solution in the presence of detergents and lipids. Anal Biochem. **138**, 141-143

49 Delano, W. L. (2006) The PyMOL Molecular Graphics System. San Carlos CA Delano Scientific

Figure Legends

Figure 1: OTUB1 crystal structure and a comparison between OTUB2 and yeast OTU1 bound to ubiquitin-Br3. **A**) Molecular surface and overlaying ribbon model of OTUB1 (residues 40-271, left panel), OTUB2 (middle panel) and yeast OTU1-ubiquitin-Br3 (right panel, ubiquitin in dark grey, OTU1 in blue) are shown. The conserved amino acids expected to be part of the catalytic center are indicated in red, blue, green and purple, respectively. **B**) A stereo view of the catalytic site regions of OTUB1 (top panel), OTUB2 (middle panel) and yeast OTU1-Ub (lower panel) illustrates hydrogen bonding networks between residues within the catalytic site. C) Display of OTUB1 (pink) and OTUB2 (yellow) as ribbon models, in which the alpha helices and beta sheets are numbered. **D**) Overlaid ribbon models of OTUB1 (pink) and yeast OTU1-UbBr3 (grey) showing the catalytic center. Catalytic site residues are indicated as in 1B, and W175 (yeast OTUB1, grey) and E214 (OTUB1, pink) are shown.

Figure 2: OTUB1 and OTUB2 reactivity towards ubiquitin probes with different C-terminal chemical groups. **A**) HA-tagged Ubiquitin equipped either with a C-terminal 2-bromoethyl (HA-Ub-Br2), 2-chloroethyl (HA-Ub-Cl2) or vinyl methylester moiety (HA-Ub-VME) was used to test the fine specificity of OTUB1 and OTUB2. **B**) Crude extracts prepared from HEK293T cells over-expressing OTUB1-HA (left panel) or OTUB2-HA (right panel) were incubated either with HA-Ub-Br2, HA-Ub-Cl2 or HA-Ub-VME, analysed by SDS-PAGE and anti-HA immunoblotting.

Figure 3: OTUB1 has a preference for cleaving lys^{48}- over lys^{63}-linked tetra-ubiquitin. **A)** Recombinant OTUB1 or cell extract was incubated with linear di-ubiquitin for 1 and 15 hours at 37°C, separated by SDS-PAGE and analysed by anti-ubiquitin immunoblotting. **B**) Recombinant OTUB1 was incubated with either lys^{48}-tetra-ubiquitin Ub_4K^{48} (top panel) or lys^{63}-linked tetra-ubiquitin Ub_4K^{63}, and cleavage monitored by SDS-PAGE and anti-Ub immunoblotting. As a control, the tetra-ubiquitin substrates were incubated either with crude cell extract or no enzyme. **C**) Ub_4K^{48} (top panel) or Ub_4K^{63} (lower panel) were incubated with recombinant OTUB1 for either 2 or 18 hours followed by time-of-flight (TOF) mass spectrometry analysis. **D**) Effect of OTUB1 on poly-ubiquitylation. HEK293T control cells or transfected with wildtype OTUB1 or C91S mutant were treated or not with the proteasome inhibitor ZL_3VS [50μM final concentration] for 4 hours at 37°C, and crude extracts analysed by SDS-PAGE and anti-Ub immunoblotting (top panel). Alternatively, crude cell extracts prepared from HEK293T control or cells expressing OTUB1 or C91S mutant were incubated with ZL_3VS [50μM final concentration] for 30min at 37°C and analysed by SDS-PAGE and anti-Ub immunoblotting. As a loading control, anti-tubulin immunoblotting was performed.

Figure 4: A) Modification of the P1' site affects cleavage of lys^{63}- and lys^{48}- linked tetra-ubiquitin by OTUB1 and OTUB2. Recombinant wildtype OTUB1, P87G mutant OTUB1, wildtype OTUB2 and G47P mutant OTUB2 were incubated with either lys^{48}- or lys^{63}-linked tetra-ubiquitin for the indicated time at 37°C. Samples were separated by SDS-PAGE and analysed by anti-ubiquitin immunoblotting. A longer exposure of the experiment performed with wildtype and P87G mutant OTUB1 is shown in the lower left panel. Anti-His immunoblotting indicates equal loading of added enzyme. **B)** Effect of P1' modifications on Ub-AMC cleavage by OTUB1 and OTUB2. 100nM Ub-AMC was incubated with wildtype or mutant G47P

OTUB2, UCH-L3, or OTUB1 at the indicated concentrations (left panel). Cleavage of Ub-AMC with wildtype or mutant P87G OTUB1 was observed at higher concentrations only (right panel). AMC cleavage was measured as a function of time by fluorescence (380/460 excitation/emission).

Figure 5: OTUB1 cleaves ubiquitin and NEDD8 conjugates, but not SUMO1/2/3 and ISG15. **A**) Ubiquitin, NEDD8, ISG15 and SUMO1 were conjugated to a biotinylated 7mer peptide and incubated with either recombinant OTUB1 or controls including UCH-L3, crude lysate or SENP2. Cleavage was monitored by SDS-PAGE and streptavidin-HRP immunoblotting. **B**) Di-SUMO2 and di-SUMO3 conjugates were incubated with recombinant OTUB1 or cell lysate as a control, and the cleavage monitored at the indicated times, followed by SDS-PAGE and anti-SUMO immunoblotting.

Figure 6: Tandem mass spectrometry based screen of OTUB1 containing protein complexes. **A**) HEK293T control cells or transfected with OTUB1 or C91S mutant were lysed either using glass beads or NP-40 detergent containing buffer, followed by an anti-HA immunoprecipitation. Isolated material was eluted from beads using TEV protease and analysed by SDS-PAGE and silver staining. Protein bands present in OTUB1 or C91S lanes and the corresponding regions in the control were subjected to LC-MS/MS analysis. 26 out of >80 proteins were found to be present only in OTUB1/C91S containing lanes; hc: heavy chain; lc: light chain. **B**) MS/MS spectra of a tryptic peptide derived from Rack1 (top panel) and a tryptic peptide derived from FUS/TLS (lower panel).

Figure 7: OTUB1 is in complex with Rack1 and FUS/TLS. **A**) OTUB1 was immunoprecipitated from HEK293T control or cells transfected with OTUB1, followed by anti-Rack1 and anti-FUS/TLS immunoblotting. **B**) OTUB1 affects the molecular weight distribution of FUS/TLS. Equal amounts of cell extracts derived from control or HEK293T cells expressing wildtype or C91S mutant OTUB1 were separated by size exclusion chromatography. Individual fractions were analysed by SDS-PAGE and immunoblotting using an anti-OTUB1 and a polyclonal anti-FUS/TLS antibody that recognizes multiple forms (left panel), or a monoclonal anti-FUS/TLS antibody that recognizes a ~60kDa form (right panel). Note that the fraction numbers are not comparable between the left and right panels. The arrow indicates the observed ~60kDa form of FUS/TLS. One out of three independent experiments is shown. **C)** HEK293T cells were transfected either with empty vector or HA-ubiquitin. Cell extracts were prepared after 24hours and subjected to anti-HA immunoprecipitation, followed by SDS-PAGE separation and analysis by anti-HA and anti-FUS immunoblotting.

Biochemical Journal Immediate Publication. Published on 27 Oct 2008 as manuscript BJ20081318

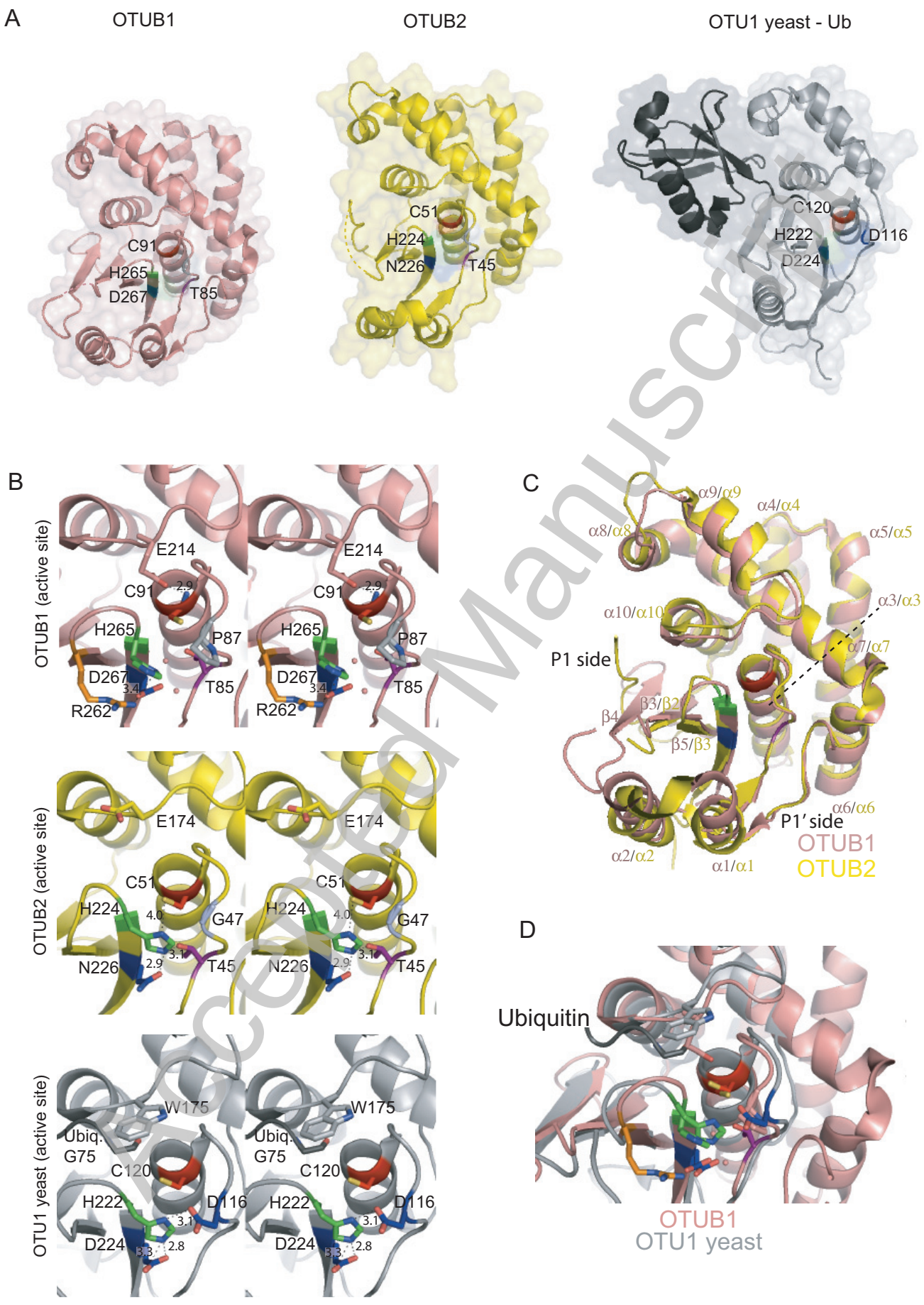

Figure 1

Biochemical Journal Immediate Publication. Published on 27 Oct 2008 as manuscript BJ20081318

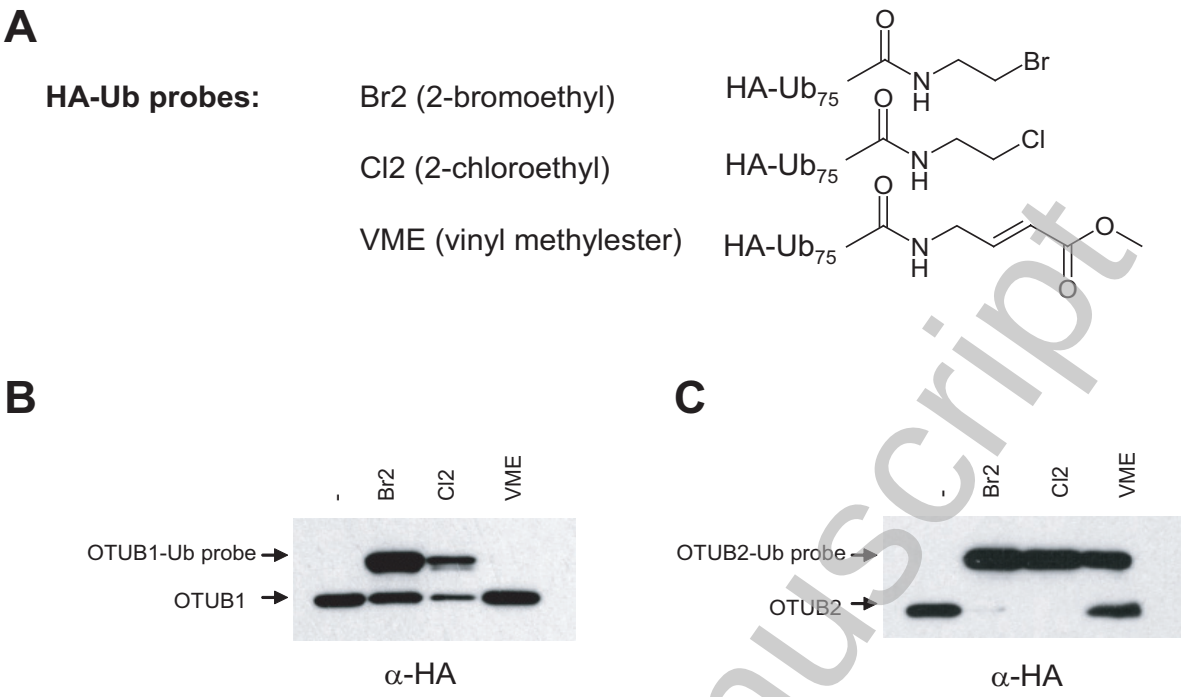

Figure 2

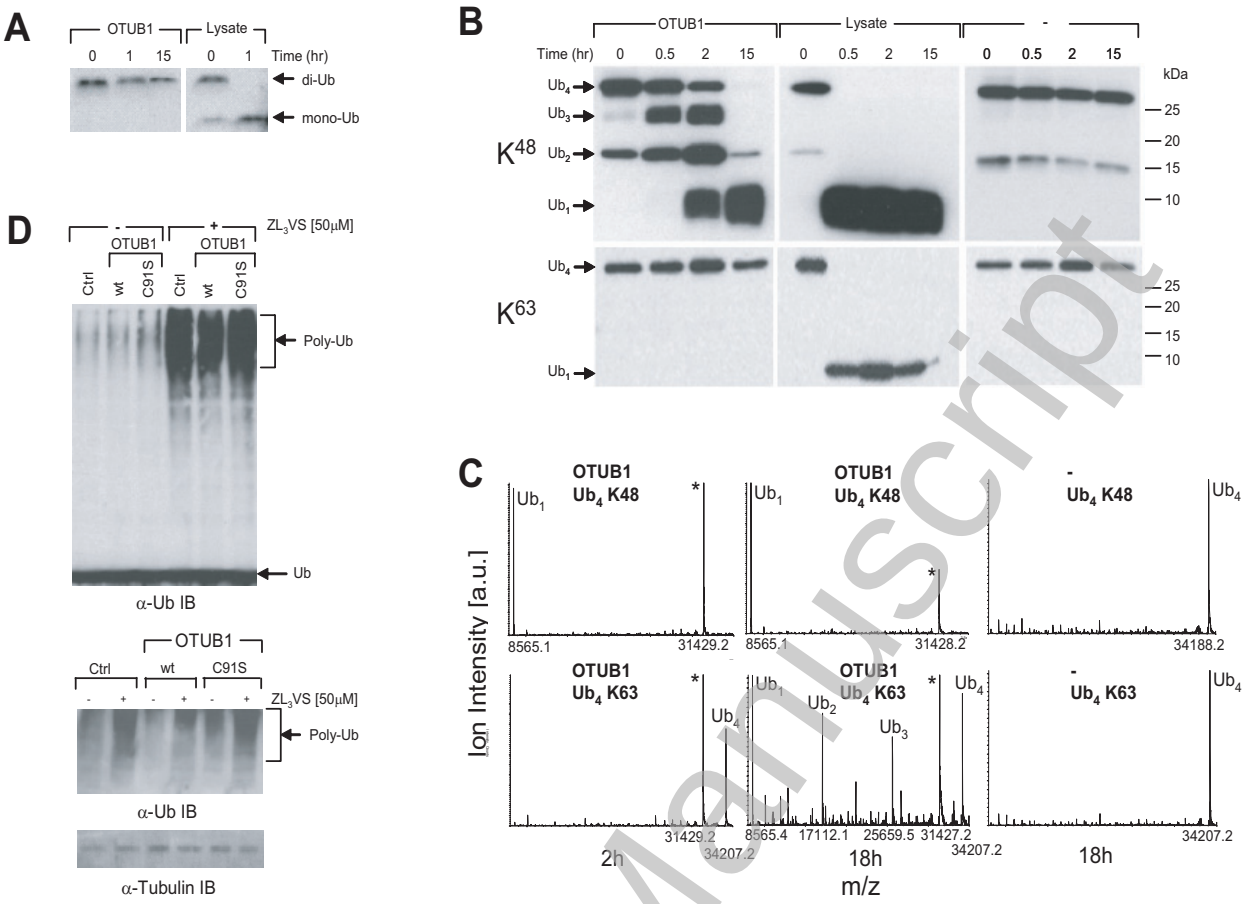

Figure 3

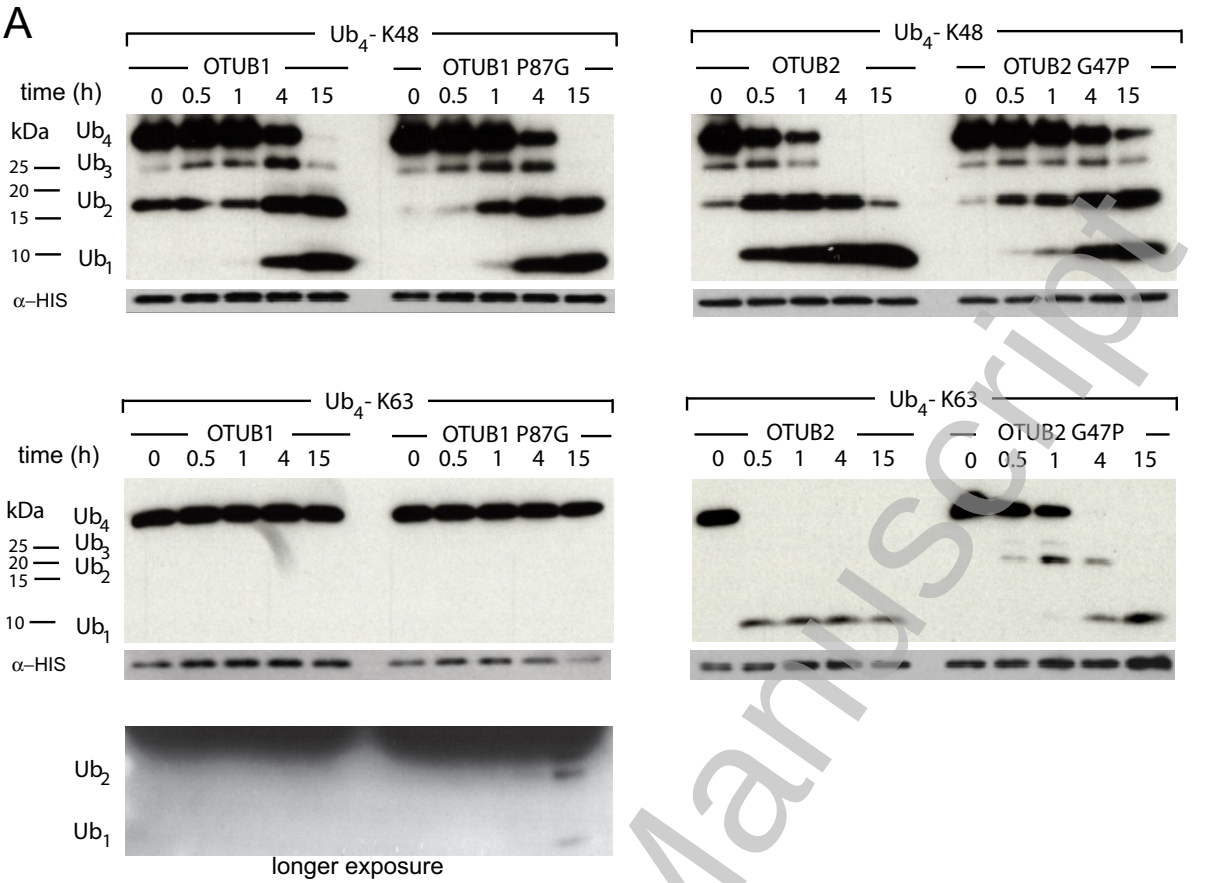

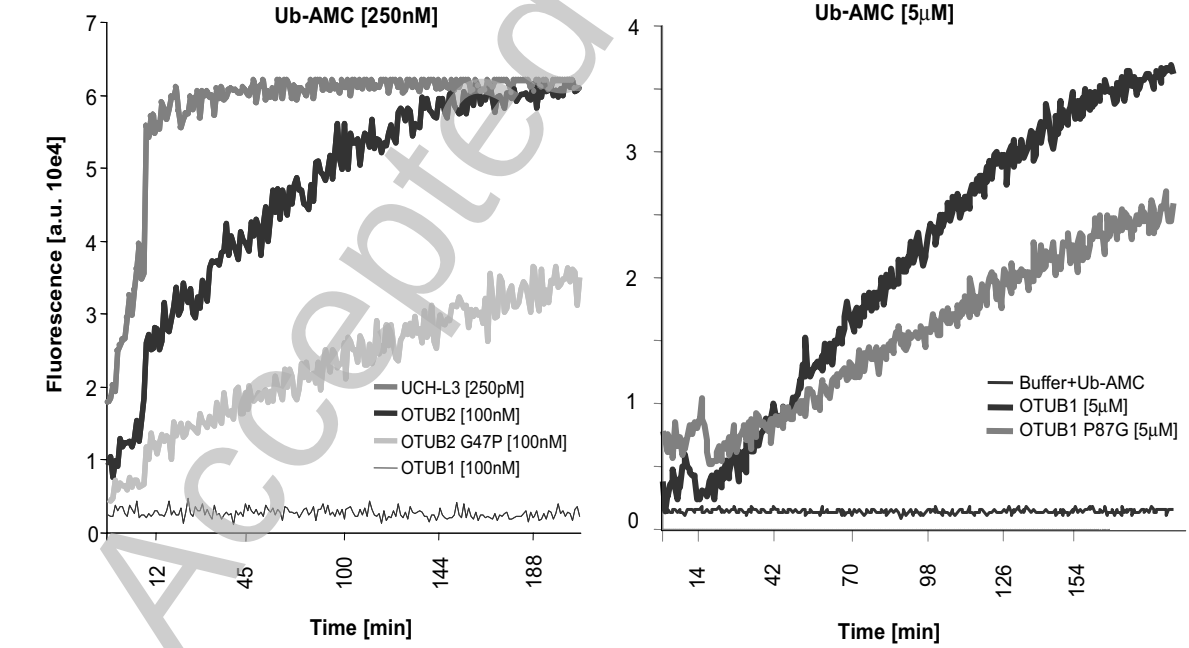

Figure 4

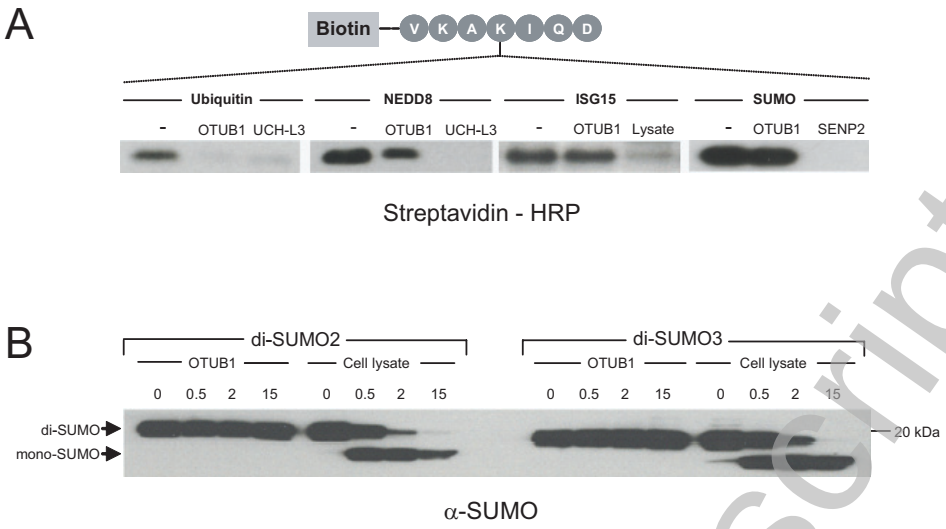

Figure 5

Biochemical Journal Immediate Publication. Published on 27 Oct 2008 as manuscript BJ20081318

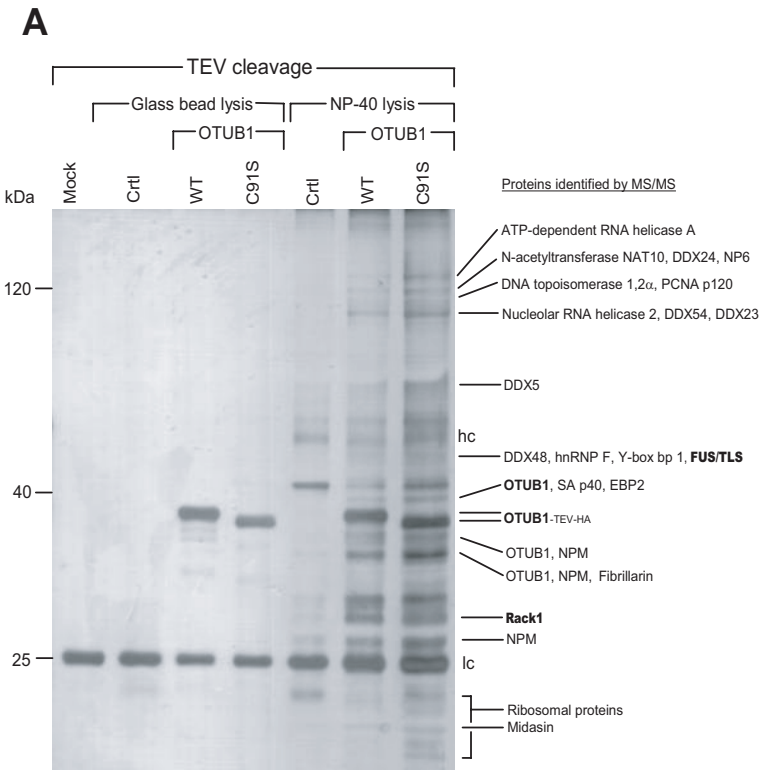

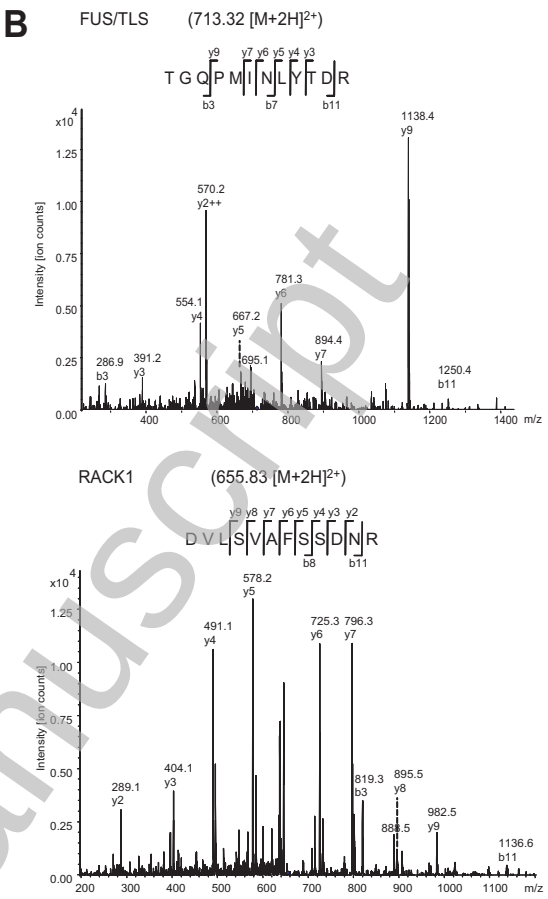

Figure 6

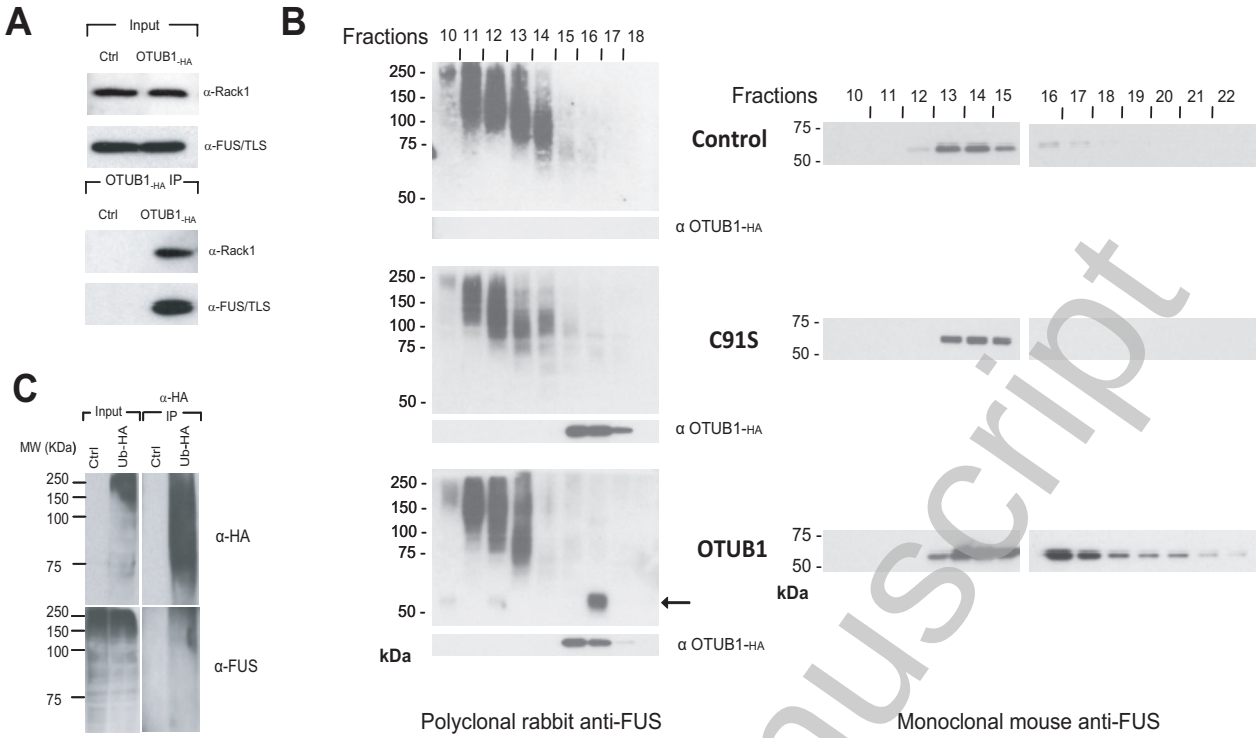

Figure 7